Emergent Continuous Symmetry in Anisotropic Flexible Two-Dimensional Materials

I. S. Burmistrov,[1,2] V. Yu. Kachorovskii,[3] M. J. Klug,[4] and J. Schmalian[4,5]
[1]L. D. Landau Institute for Theoretical Physics, Semenova 1-a, 142432 Chernogolovka, Russia
[2]Laboratory for Condensed Matter Physics, HSE University, 101000 Moscow, Russia
[3]A. F. Ioffe Physico-Technical Institute, 194021 St. Petersburg, Russia
[4]Institute for Theory of Condensed Matter, Karlsruhe Institute of Technology, 76131 Karlsruhe, Germany
[5]Institute for Quantum Materials and Technologies, Karlsruhe Institute of Technology, 76131 Karlsruhe, Germany

(Received 22 August 2021; revised 16 December 2021; accepted 9 February 2022; published 1 March 2022)

We develop the theory of anomalous elasticity in two-dimensional flexible materials with orthorhombic crystal symmetry. Remarkably, in the universal region, where characteristic length scales are larger than the rather small Ginzburg scale ∼10 nm, these materials possess an infinite set of flat phases. These phases corresponds to a stable line of fixed points and are connected by an emergent continuous symmetry. This symmetry enforces power law scaling with momentum of the anisotropic bending rigidity and Young's modulus, controlled by a single universal exponent—the very same along the whole line of fixed points. These anisotropic flat phases are uniquely labeled by the ratio of absolute Poisson's ratios. We apply our theory to phosphorene.

DOI: 10.1103/PhysRevLett.128.096101

The discovery of graphene [1–3] and closely related atomically thick materials [4] led to the field of flexible two-dimensional (2D) materials [5]. The hexagonal crystal symmetry of graphene results in elastic and electronic transport properties identical to those of isotropic systems. More recently, research has shifted towards other 2D materials, including 2D black phosphorus (phosphorene) [6,7], transition metal dichalcogenide monolayers [8,9], and metal monochalcogenide monolayers [10,11]. Because of their different crystal structure, these 2D materials demonstrate anisotropic physical properties, such as electron and thermal transport, optical absorption, photoluminescence, Raman scattering, and—as will be important in this Letter—elastic response. In particular, for 2D materials with orthorhombic crystal symmetry, e.g., boat and washboard graphane [12], phosphorene, metal monochalcogenide monolayers (SiS, SiSe, GeS, GeSe, SnS, and SnSe), monolayers $GeAs_2$, WTe_2, $ZrTe_5$, Ta_2NiS_5, etc. [13], the elastic free energy *does not* reduce to that of an isotropic crystalline membrane and results in anisotropic Young's moduli and Poisson's ratios.

The idea of anomalous elasticity of isotropic crystalline membranes dates back to the seminal work by Nelson and Peliti [14]. Later it was found that the competition between anomalous elasticity and thermal fluctuations in clean membranes leads to the existence of a transition from a flat to a crumpled phase with increasing temperature, T [15–20]. There is still substantial interest in furthering our understanding of clean membranes [21–31].

In this Letter we develop the theory of anomalous elasticity of 2D membranes with orthorhombic crystal symmetry. Our theory is focused on the universal regime when the typical size L of the membrane is large in comparison with the so-called Ginzburg scale, q_*^{-1} (see below). As we show, for the mentioned 2D materials $q_*^{-1} \sim 10$ nm is extremely small, making the universal regime highly relevant.

The theory of anomalous elasticity predicts that, in the universal regime, $L \gg q_*^{-1}$, the physical properties of isotropic 2D membranes are determined by the dimensionless ratio of the bending rigidity $\varkappa$ and the temperature T. In the flat phase of the membrane, this parameter exhibits power-law scaling behavior with the system size $\varkappa/T \propto L^{\eta}$. It behaves as a coupling constant or effective charge of a renormalizable theory. A universal exponent η depends solely on the dimensions of the membrane D and of the embedding space d, respectively [17]. The situation of physical interest is, of course, $D = 2$ and $d = 3$. The physics of an *anisotropic* membrane, where the bending rigidity $\varkappa_{\alpha\beta}$ becomes a symmetric tensor, with $\alpha, \beta \in \{x, y\}$, is then described by several effective charges. Hence, the degree and the nature of the anisotropy can change as one probes phenomena on different length scales. An analysis in $D = 4 - \epsilon$ with $\epsilon \ll 1$ yields that the membrane becomes asymptotically isotropic: $\varkappa_{\alpha\beta} \to \varkappa\delta_{\alpha\beta}$ for $L \to \infty$ [32]. We show this is not the case for the physically relevant case of an orthorhombic crystalline membrane with $D = 2$. We demonstrate that in the universal regime such a membrane has a discrete hidden symmetry preserving the degree of orthorhombicity, $\gamma \equiv (\varkappa_{xx}/\varkappa_{yy})^{1/4}$. At $L \to \infty$ this discrete symmetry transforms into an emergent continuous symmetry that controls anisotropy effects of orthorhombic 2D membranes. The latter are not captured by the frequently used ϵ-expansion near dimension $D = 4$.

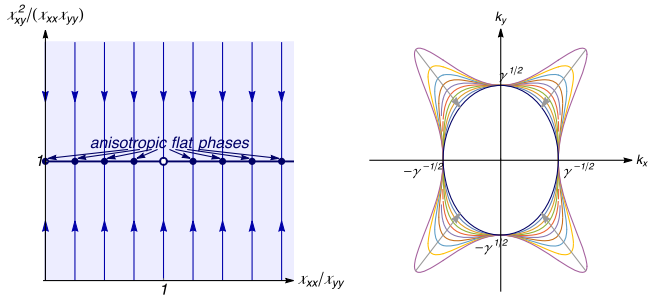

FIG. 1. Left: Sketch of the RG flow (arrows indicate direction of increase of a system size L). Anisotropic flat phases on the line of fixed points are marked by blue dots. The isotropic flat phase is indicated by the white point. Right: The contour plot of schematic change of the normalized bending rigidity $k^4\varkappa(\theta_{\boldsymbol{k}})/\sqrt{\varkappa_{xx}\varkappa_{yy}}$ under the RG flow for $\varkappa_{xx} > \varkappa_{yy}$, Eq. (5). For $\varkappa_{xx} < \varkappa_{yy}$ one needs to interchange the axes k_x and k_y.

More specifically, we predict that for $L \gg q_*^{-1}$, in contrast to graphene and dichalcogenide monolayers, orthorhombic 2D materials possess an *infinite set* of flat phases with universal size-dependent elastic properties preserving the orthorhombic anisotropy. Remarkably, all these phases are connected to the flat state of an isotropic membrane by the *emergent continuous symmetry*.

The latter ensures that for all phases the anisotropic anomalous Hooke's law is controlled by the same exponent η known from isotropic membranes [33]. Analyzing the effective interaction of soft flexural phonons, these results are obtained from renormalization group (RG) equations that govern scaling of the bending rigidity tensor with L. We obtain a *line of stable fixed points* that describes the infinite set of anisotropic flat phases, corresponding to different parameters γ (see Fig. 1). In all cases the angular-dependent bending rigidity, $\varkappa(\theta_{\boldsymbol{k}}) = \varkappa_{\alpha\beta}\hat{k}_\alpha^2\hat{k}_\beta^2$, with $\hat{\boldsymbol{k}} = (\cos\theta_{\boldsymbol{k}}, \sin\theta_{\boldsymbol{k}})$ the unit vector along the momentum $\boldsymbol{k}$, flows to an elliptic dependence on $\theta_{\boldsymbol{k}}$ controlled by γ. The power law scaling with k is then governed by the exponent η (see Fig. 1 and Eqs. (5)). Finally, we study the transition to a tubular phase, where an anisotropic 2D membrane is crumpled along one direction [32,34–37]. While we show that for a generic anisotropic membrane such a transition should formally occur with increasing T, for 2D materials listed above it happens at unphysically high temperatures (of the order of tens of eV).

Model.—Following Ref. [32], the free energy describing thermal fluctuations in the flat phase of a 2D membrane with orthorhombic crystal symmetry can be written as $\mathcal{F} = \int d^2\boldsymbol{x}\varkappa_{\alpha\beta}^{(0)}(\nabla_\alpha^2\boldsymbol{r})(\nabla_\beta^2\boldsymbol{r})/2 + \mathcal{F}_{\rm el}$. Here, $\boldsymbol{r}$ is a $d = d_c + 2$ dimensional vector parametrizing the membrane and $\varkappa_{\alpha\beta}^{(0)}$ is bare bending rigidity. The elastic crystalline energy, $\mathcal{F}_{\rm el} = \int d^2\boldsymbol{x}[c_{11}u_{xx}^2 + c_{22}u_{yy}^2 + 2c_{12}u_{xx}u_{yy} + 4c_{66}u_{xy}^2]/2$, is expressed via the strain tensor $u_{\alpha\beta} = (\partial_\alpha\boldsymbol{r}\partial_\beta\boldsymbol{r} - \delta_{\alpha\beta})/2$. Here $\{c_{\alpha\beta}, c_{66}\}$ are the elastic moduli of orthorhombic 2D crystalline material. For physical membranes $d_c = 1$, while anharmonic effects can be efficiently described in terms of a standard expansion in $1/d_c$ [17].

In the case of $\varkappa_{xx}^{(0)} = \varkappa_{yy}^{(0)}$ and $c_{11} = c_{22}$, the tetragonal crystal symmetry holds. For graphene which has hexagonal symmetry, the bending energy is isotropic, $\varkappa_{xx}^{(0)} = \varkappa_{yy}^{(0)} = \varkappa_{xy}^{(0)}$ together with $c_{11} = c_{22} = c_{12} + 2c_{66}$.

We use the parametrization of the coordinates: $r_1 = \xi_x x + u_x$, $r_2 = \xi_y y + u_y$, and $r_{a+2} = h_a$ with $a = 1, \ldots, d_c$. The vectors $\boldsymbol{u} = \{u_x, u_y\}$ and $\boldsymbol{h} = \{h_1, \ldots, h_{d_c}\}$ stand for in-plane and out-of-plane displacements, respectively. Following Ref. [14], we focus on nonlinear elastic contributions of the flexural, out-of-plane displacements $\boldsymbol{h}$, integrate out $\boldsymbol{u}$, and obtain the effective free energy written in terms of the out-of-plane phonons only: $\mathcal{F} = \int\{dk\}\varkappa_0(\theta_{\boldsymbol{k}})k^4\boldsymbol{h}_{\boldsymbol{k}}\boldsymbol{h}_{-\boldsymbol{k}}/2 + \mathcal{F}_{\rm int}$. The term [38]

$$\mathcal{F}_{\rm int} = \frac{1}{8}\int'\{dq\}Y_0(\theta_{\boldsymbol{q}})\left|\int\{dk\}[\boldsymbol{k}\times\hat{\boldsymbol{q}}]^2\boldsymbol{h}_{\boldsymbol{k}+\boldsymbol{q}}\boldsymbol{h}_{-\boldsymbol{k}}\right|^2, \quad (1)$$

is responsible for effective h^4 interaction of the flexural modes. Here we define $\{dk\} = d^2\boldsymbol{k}/(2\pi)^2$. The bare interaction of the h modes is anisotropic and determined by the direction-dependent Young's modulus $Y_0(\theta_{\boldsymbol{q}})$ [39,40].

Because of anharmonic flexural phonon interactions, the bare coupling $Y_0(\theta_{\boldsymbol{q}})$ is screened, and the bending rigidity tensor is subject to renormalization, $\varkappa_{\alpha\beta}^{(0)} \to \varkappa_{\alpha\beta}$, an effect that can be described with three running coupling constants that we write as

$$\gamma = (\varkappa_{xx}/\varkappa_{yy})^{1/4}, \quad \tilde{\varkappa} = \sqrt{\varkappa_{xx}\varkappa_{yy}}, \quad t = \frac{\tilde{\varkappa} - \varkappa_{xy}}{3\tilde{\varkappa} + \varkappa_{xy}}. \quad (2)$$

The asymmetry between x and y axes is controlled by γ with $\gamma = 1$ for tetragonal systems. t describes the tetragonal distortion of the membrane's bending energy. $\tilde{\varkappa}$ is the geometric mean bending rigidity. To ensure that $\varkappa(\theta) > 0$, we consider $0 < \gamma < \infty$ and $|t| < 1$.

Renormalization.—To solve the anharmonic problem it is convenient to work in the rescaled coordinates,

$$x = x'\sqrt{\gamma}, \quad y = y'/\sqrt{\gamma}, \quad k_x = k_x'/\sqrt{\gamma}, \quad k_y = k_y'\sqrt{\gamma}, \quad (3)$$

in which the bending energy acquires the tetragonal form, $\varkappa(\theta) \mapsto \tilde{\varkappa}(\theta) = \tilde{\varkappa}[1 + t\cos(4\theta)]/(1+t)$. Note, even after rescaling the Young's modulus $\tilde{Y}_0(\theta)$ (and $\mathcal{F}$) still depends on γ.

The necessary information can be extracted from the correlation function $\langle h_a(\boldsymbol{k})h_b(-\boldsymbol{k})\rangle \equiv \mathcal{G}_{\boldsymbol{k}}\delta_{ab}$ of the flexural phonons. We have $\mathcal{G}_{\boldsymbol{k}} = T/[\tilde{\varkappa}_0(\theta_{\boldsymbol{k}})k^4]$ without anharmonicity. The bare interaction $\tilde{Y}_0(\theta)$ gets screened by multiple anharmonic scattering events that can be analyzed in terms of RPA diagrams [see Fig. 2(a)]. Just like for the isotropic case, the screened Young's modulus $\tilde{Y}(\theta)$

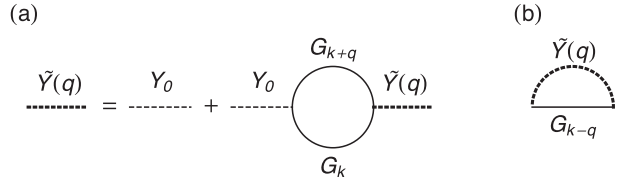

FIG. 2. (a) The RPA-type resummation for the Young's modulus. (b) The self-energy correction to first order in $1/d_c$. The solid line represents the bare Green's function $G_{\boldsymbol{k}}$. The thin (thick) dashed line denotes the bare (screened) interaction.

becomes independent of $\tilde{Y}_0(\theta)$ in the universal regime, $q \ll q_* \sim [d_c Y_0 T/\varkappa_{xx}^{(0)}\varkappa_{yy}^{(0)}]^{1/2}$. Then, the remaining γ dependence of the bare Young's modulus $\tilde{Y}_0(\theta)$ gets eliminated by screening effects, so that γ drops out of the analysis completely and no longer gets renormalized. In turn, the anisotropic screened interaction $\tilde{Y} \sim q^2$ gives rise to a renormalization of the bending rigidity that enters $\mathcal{G}_{\boldsymbol{k}} = T/[\tilde{\varkappa}(\theta_{\boldsymbol{k}})k^4]$ [see Fig. 2(b)]. This analysis can be efficiently captured in terms of one loop RG flow equations (see Supplemental Material [41]):

$$\frac{d\gamma}{d\Lambda} = 0, \qquad \frac{dt}{d\Lambda} \simeq -\frac{2}{d_c} g(t), \qquad \frac{d\ln\tilde{\varkappa}}{d\Lambda} \simeq \frac{2}{d_c}\chi(t), \tag{4}$$

where $\Lambda = \ln(q_*/k)$ and q_* plays a role of the ultraviolet scale at which initial values of coupling constants are defined: $\gamma(0) = \gamma$, $t(0) = t_0$, and $\tilde{\varkappa}(0) = \tilde{\varkappa}_0$. We stress that the first of the RG Eqs. (4) is *exact* rather than limited to the one loop approximation [41]. Following Ref. [42], we introduce the momentum-dependent stretching factor, $\xi_\alpha^2(k) = 1 - d_c \int_k \{dq\} q_\alpha^2 \mathcal{G}_{\boldsymbol{q}}$ that includes contributions from the flexural phonons with momenta larger than a given momentum k (in the rescaled coordinates), $\gamma q_x^2 + q_y^2/\gamma > k^2$.

The functions $g(t)$ and $\chi(t)$ are shown in Fig. 3. The odd function $g(t)$ ensures that t always flows to zero, such that $\varkappa_{xy} \to (\varkappa_{xx}\varkappa_{yy})^{1/2}$ at long length scales. While this is also obeyed in a tetragonal system, our long distance behavior is by no means effectively tetragonal as $\varkappa_{xx}/\varkappa_{yy}$ does not flow to unity. The parameter γ is not renormalized and, thus, determines an entire line of fixed points.

For small but finite t, it holds $g(t) \simeq (65t/54) + O(t^3)$ and $\chi(t) \simeq 1 - (65t/54) + (145t^2/162) + O(t^3)$ (see Fig. 3). Hence, the bending rigidity scales just like for isotropic membranes at the infrared stable line of fixed points: $\tilde{\varkappa} \sim (q_*/k)^\eta$ where $\eta \simeq 2/d_c$. The line of fixed points is reached asymptotically according to $t \sim (k/q_*)^\psi$, with $\psi \simeq 65/(27 d_c)$. This crossover exponent controls the rate at which $\varkappa(\theta)$ approaches the elliptical form; see Fig. 1.

We stress that the line of fixed points is unique to 2D membranes. For membranes of higher dimensions, $D > 2$, we find that $d\gamma/d\Lambda = -A_D(D-2)(\gamma-1)/d_c$ for $|\gamma - 1| \ll 1$ [41]. Since $A_D > 0$, a weak crystalline

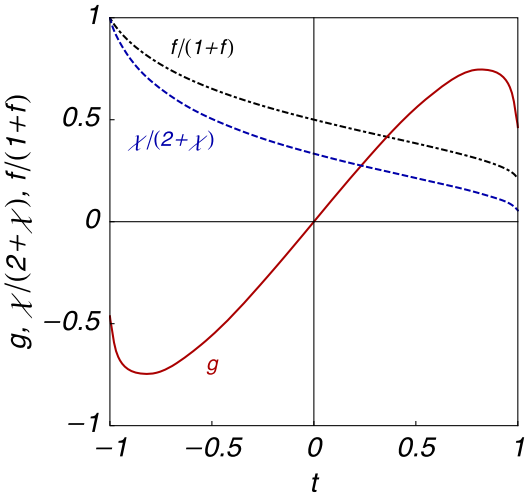

FIG. 3. The functions $g(t)$ and $\chi(t)$, that enter the RG Eqs. (4), and the function $f(t)$ that determines transition temperature to the tubular phase are shown.

anisotropy is irrelevant at long length scales unless $D = 2$, in accordance with RG analysis for $D = 4 - \epsilon$ [32].

Beyond one loop.—The existence of the line of fixed points at $t = 0$ does not rely on the one loop approximation. Generically, it is natural to assume that (i) the line of fixed points remains stable ($\psi > 0$), (ii) there are no higher order harmonics in $\tilde{\varkappa}(\theta)$ are generated under the RG flow, (iii) $t = 0$ is the only fixed point for $|t| < 1$. Then, the elasticity of 2D membranes with the orthorhombic crystal symmetry in the universal regime can be deduced from scaling (with rescaled momentum) of bending rigidity, $\tilde{\varkappa} \sim (q_*/k)^\eta$, and Young's modulus, $\tilde{Y} \sim (k/q_*)^{2-2\eta}$ as for isotropic membranes [15]. Making inverse rescaling to the original coordinates, Eq. (3), we find in the infrared (IR) limit (as $t \to 0$):

$$\begin{aligned} \varkappa_{\rm IR}(\boldsymbol{k}) &\sim (\gamma\cos^2\theta_{\boldsymbol{k}} + \gamma^{-1}\sin^2\theta_{\boldsymbol{k}})^{2-\eta/2}(q_*/k)^\eta, \\ Y_{\rm IR}(\boldsymbol{k}) &\sim [(\gamma\cos^2\theta_{\boldsymbol{k}} + \gamma^{-1}\sin^2\theta_{\boldsymbol{k}})k^2/q_*^2]^{1-\eta}. \end{aligned} \tag{5}$$

The scaling of $\varkappa_{\rm IR}$ and $Y_{\rm IR}$ with the absolute value of momentum is controlled by the critical exponent η, known for the isotropic membrane. For $d_c \gg 1$ it is given as $\eta = 2/d_c + [73 - 68\zeta(3)]/(27 d_c^2) + O(1/d_c^3)$ [28], whereas for $d_c = 1$ the numerics predicts $\eta = 0.795 \pm 0.01$ [43].

Remarkably, $\varkappa_{\rm IR}(\boldsymbol{k})k^4$ and $Y_{\rm IR}(\boldsymbol{k})$ obey a continuous symmetry under the affine transformation $\boldsymbol{k} \to R_\varphi^{-1}\boldsymbol{k}$, where

$$R_\varphi = \begin{pmatrix} \cos\varphi & \gamma^{-1}\sin\varphi \\ -\gamma\sin\varphi & \cos\varphi \end{pmatrix}. \tag{6}$$

This is just the symmetry of the ellipse shown in Fig. 1. The same continuous symmetry ($\boldsymbol{x} \to R_\varphi \boldsymbol{x}$) emerges for the free energy $\mathcal{F}$ at the line of fixed points in the same IR limit, $t = 0$. We emphasize that the continuous symmetry (6) is

the *emergent* one. In the universal region, $q < q_*$, and for any nonzero t, $\mathcal{F}$ has the discrete symmetry $R_{\pi/2}$ only (also seen from Fig. 1). This discrete symmetry is responsible for keeping γ unrenormalized.

Anomalous elasticity.—Under application of a tension σ to an isotropic membrane, the power-law scaling of elastic moduli with momentum is limited by $k_\sigma \sim \sigma^{1/(2-\eta)}$ which is determined from the relation $\tilde{\varkappa}(k_\sigma)k_\sigma^2 \sim \sigma$. This leads to an anomalous Hooke's law for tension-induced deformations, $\delta\xi^2 \sim \sigma/\tilde{Y}(k_\sigma) \sim \sigma^\alpha$ with $\alpha = \eta/(2-\eta)$ [18,19]. Performing the inverse of the rescaling (3), we find the deformations along the x and y axes due to an unidirectional tension σ_x as [41]

$$\delta\xi_x^2 \sim \gamma^{-1}(\sigma_x/\gamma)^\alpha, \qquad \delta\xi_y^2 \sim \gamma(\sigma_x/\gamma)^\alpha. \tag{7}$$

Although the mechanics of a membrane on the line of the fixed points remains anisotropic, the anomalous Hooke's law (7) is controlled by the same exponent α as for isotropic membranes.

As expected, the membrane is deformed easier in the direction for which the bending rigidity is smaller. For example, from Eq. (7) it follows that $\delta\xi_y^2 > \delta\xi_x^2$ for $\gamma > 1$ ($\varkappa_{xx}^{(0)} > \varkappa_{yy}^{(0)}$). We note that the power-law behavior (7) holds for $\sigma_x \ll \sigma_* \sim \tilde{\varkappa}_0 q_*^2$. The results for unidirectional tension along the y axis can be obtained from Eq. (7) under the interchange $x \leftrightarrow y$ and $\gamma \leftrightarrow 1/\gamma$.

The anomalous Hooke's law (7) results in an anisotropic *negative* absolute Poisson's ratio. In the anisotropic flat phase one finds for $\sigma_x, \sigma_y \ll \sigma_*$,

$$\nu_x = -\frac{\delta\xi_y^2(\sigma_x)}{\delta\xi_x^2(\sigma_x)} = \gamma^2\nu, \qquad \nu_y = -\frac{\delta\xi_x^2(\sigma_y)}{\delta\xi_y^2(\sigma_y)} = \frac{\nu}{\gamma^2}. \tag{8}$$

Here, $\nu = -1 + 2/d_c - a/d_c^2 + O(1/d_c^3)$ with $a \approx 1.76 \pm 0.02$ denotes the absolute Poisson's ratio for the isotropic membrane [28]. Since $\nu_x/\nu_y = \gamma^4$, the measurement of the absolute Poisson's ratios in the regime of anomalous Hooke's law, $\sigma_x, \sigma_y \ll \sigma_*$, allows one to uniquely characterize the anisotropy in the bending rigidity.

Tubular phase.—The dependence $\xi_x^2(k)$ can be cast in the form of the RG equation,

$$\frac{d\xi_x^2}{d\Lambda} = -\frac{d_c T}{4\pi\varkappa_{xx}^{3/4}\varkappa_{yy}^{1/4}}\left(\frac{1+t}{1-t}\right)^{1/2}, \qquad \xi_x^2(\Lambda = 0) = 1. \tag{9}$$

The RG equation for ξ_y^2 can be obtained from Eq. (9) by interchanging x and y. At low temperatures the flat phase, in which $\xi_\alpha^2(k)$ is positive for all $k < q_*$, is realized. For $\gamma < 1$, with increase of temperature $\xi_x^2(k)$ vanishes at some finite value of k. At the same time $\xi_y^2(k)$ is still positive for all $k < q_*$. Therefore, the tubular phase exists above the transition temperature $T_x = T_x^{(0)} f(t_0)$ where $T_x^{(0)} = (8\pi/d_c^2)[\varkappa_{xx}^{(0)3}\varkappa_{yy}^{(0)}]^{1/4}$ stands for the temperature of the crumpling transition at $t_0 = 0$. The crumpling occurs along the direction x that corresponds to the smaller bare bending rigidity, $\varkappa_{xx}^{(0)} < \varkappa_{yy}^{(0)}$. The function $f(t)$ can be found from RG equations (4) and (9) [41]. It is a monotonically decreasing function with $f(t \to -1) \sim (1+t)^{-1}$, $f(0) = 1$, and $f(1) \approx 0.3$; see Fig. 3. Further increasing temperature the tubular phase experiences a crumpling transition [34,36]. For $\gamma < 1$ the tubular phase at $T > T_y$ corresponds to $\xi_y^2(k = 0) = 0$. The transition temperature T_y can be obtained from the expression for T_x upon interchange x and y.

Discussion.—As an illustration of our theory we apply it to 2D black phosphorus. We are not aware of direct measurements of elastic and bending moduli of phosphorene. Recent numerical calculations report $c_{11} \approx 105.2$, $c_{22} \approx 26.2$, $c_{12} \approx 18.4$, and $c_{66} \approx 22.4$ (measured in N/m) [44] as well as $\varkappa_{xx}^{(0)} \approx 8.0$ and $\varkappa_{yy}^{(0)} \approx 4.8$ eV [45]. This yields $q_*^{-1} \approx 10$ nm. Hence, anomalous elasticity should always dominate the anisotropic elastic properties of available experimentally samples.

For 2D black phosphorus our theory predicts that the nonlinear Hooke's law, Eq. (7), and negative absolute Poisson's ratios, Eq. (8), should be observable for tensions smaller than $\sigma_* \approx 0.01$ N/m. Although we are not aware of measurements of strain-stress dependence of phosphorene we believe that it can be performed in a way similar to graphene [46]. There are several computations of the Poisson's ratios for black phosphorus from first principles [47,48]. While these results yield a negative Poisson's ratios of phosphorene, the numerical computation of the Poisson's ratio in the regime of low applied tensions, $\sigma_{x,y} \ll \sigma_*$, may suffer from a problem with proper boundary conditions in a finite size sample [27]. As in the case of graphene, a direct measurement of the Poisson's ratio of phosphorene is challenging. We estimate the transition temperature to the tubular phase, $T_x^{(0)}$, to be of the order of 50 eV, i.e., the anisotropic flat phase of phosphorene is stable for all experimentally relevant T.

We also note that results (5) for the effective bending rigidity and Young's modulus are important for an electron transport in 2D materials. Recently, the anisotropy of the carrier mobility of 2D black phosphorus was studied using an effective bending rigidity of precisely the asymptotic form of Eq. (5) [49,50].

It is worthwhile mentioning that recently a distinct anisotropic model which breaks the $O(d)$ rotational invariance in the embedded space has been studied [51]. It would be interesting to analyze the effects of crystalline anisotropy, discussed above, for the model of Ref. [51].

To summarize, we developed a theory of anomalous elasticity in systems with orthorhombic crystal symmetry, relevant for a large number of recently studied 2D flexible materials. Our key finding is a discrete symmetry of the

theory, existing in the universal regime and leading to an infinite number of anisotropic flat phases in the long-wave limit.

Remarkably, this result is specific for physical membranes with $D = 2$. The infrared physics of these flat phases is controlled by the emergent continuous symmetry that connects them to the flat phase of isotropic membrane. The flat phases have an anisotropic bending rigidity and Young's modulus whereas the scaling with momentum is the same as in the isotropic case. They are uniquely labeled by the ratio of absolute Poisson's ratios in the two perpendicular directions. Our theory can easily be extended to even less symmetric 2D materials with triclinic and monoclinic crystal symmetries, e.g., monolayers ReS_2, $ReSe_2$, GaTe, GeP, GeAs, SiP, SiAs, etc. Also, the effects of in-plane and curvature disorder [25,29,42,52–61] can be considered. The later was shown to be important for a quantitative explanation of nonlinear strain-stress relation in graphene [59].

We thank M. Glazov and V. Lebedev for useful comments and discussions. The work was funded in part by the Alexander von Humboldt Foundation, by the Russian Ministry of Science and Higher Educations, the Basic Research Program of HSE, by the Russian Foundation for Basic Research, Grant No. 20-52-12019, and by the Deutsche Forschungsgemeinschaft (DFG, German Research Foundation) project SCHM 1031/12-1.

[1] K. S. Novoselov, A. K. Geim, S. V. Morozov, D. Jiang, Y. Zhang, S. V. Dubonos, I. V. Grigorieva, and A. A. Firsov, Electric field effect in atomically thin carbon films, Science **306**, 666 (2004).

[2] K. S. Novoselov, A. K. Geim, S. V. Morozov, D. Jiang, M. I. Katsnelson, I. V. Grigorieva, S. V. Dubonos, and A. A. Firsov, Two-dimensional gas of massless Dirac fermions in graphene, Nature (London) **438**, 197 (2005).

[3] Y. Zhang, Y.-W. Tan, H. L. Stormer, and P. Kim, Experimental observation of the quantum Hall effect and Berry's phase in graphene, Nature (London) **438**, 201 (2005).

[4] K. S. Novoselov and A. H. Castro Neto, Two-dimensional crystals-based heterostructures: Materials with tailored properties, Phys. Scr. **T146**, 014006 (2012).

[5] *2D Materials: Properties and Devices*, edited by P. Avouris, T. F. Heinz, and T. Low (Cambridge University Press, Cambridge, England, 2017).

[6] X. Ling, H. Wang, S. Huang, F. Xia, and M. S. Dresselhaus, The renaissance of black phosphorus, Proc. Natl. Acad. Sci. U.S.A. **112**, 4523 (2015).

[7] M. Galluzzi, Y. Zhang, and X.-F. Yu, Mechanical properties and applications of 2d black phosphorus, J. Appl. Phys. **128**, 230903 (2020).

[8] G. Wang, A. Chernikov, M. M. Glazov, T. F. Heinz, X. Marie, Th. Amand, and B. Urbaszek, Colloquium: Excitons in atomically thin transition metal dichalcogenides, Rev. Mod. Phys. **90**, 021001 (2018).

[9] M. V. Durnev and M. M. Glazov, Excitons and trions in two-dimensional semiconductors based on transition metal dichalcogenides, Phys. Usp. **61**, 825 (2018).

[10] A. S. Sarkar and E. Stratakis, Recent advances in 2D metal monochalcogenides, Adv. Sci. **7**, 2001655 (2020).

[11] S. Barraza-Lopez, B. M. Fregoso, J. W. Villanova, S. S. P. Parkin, and K. Chang, Colloquium: Physical properties of group-IV monochalcogenide monolayers, Rev. Mod. Phys. **93**, 011001 (2021).

[12] L. Colombo and S. Giordano, Nonlinear elasticity in nanostructured materials, Rep. Prog. Phys. **74**, 116501 (2011).

[13] L. Li, W. Han, L. Pi, P. Niu, J. Han, C. Wang, B. Su, H. Li, J. Xiong, Y. Bando, and T. Zhai, Emerging in-plane anisotropic two-dimensional materials, InfoMat **1**, 54 (2019).

[14] D. R. Nelson and L. Peliti, Fluctuations in membranes with crystalline and hexatic order, J. Phys. (Paris) **48**, 1085 (1987).

[15] J. A. Aronovitz and T. C. Lubensky, Fluctuations of solid membranes, Phys. Rev. Lett. **60**, 2634 (1988).

[16] M. Paczuski, M. Kardar, and D. R. Nelson, Landau Theory of the Crumpling Transition, Phys. Rev. Lett. **60**, 2638 (1988).

[17] F. David and E. Guitter, Crumpling transition in elastic membranes: Renormalization group treatment, Europhys. Lett. **5**, 709 (1988).

[18] J. Aronovitz, L. Golubovic, and T. C. Lubensky, Fluctuations and lower critical dimensions of crystalline membranes, J. Phys. (Paris) **50**, 609 (1989).

[19] E. Guitter, F. David, S. Leibler, and L. Peliti, Thermodynamical behavior of polymerized membranes, J. Phys. (Paris) **50**, 1787 (1989).

[20] P. Le Doussal and L. Radzihovsky, Self-Consistent Theory of Polymerized Membranes, Phys. Rev. Lett. **69**, 1209 (1992).

[21] E. I. Kats and V. V. Lebedev, Asymptotic freedom at zero temperature in free-standing crystalline membranes, Phys. Rev. B **89**, 125433 (2014).

[22] E. I. Kats and V. V. Lebedev, Erratum: Asymptotic freedom at zero temperature in free-standing crystalline membranes [Phys. Rev. B **89**, 125433 (2014)]; Phys. Rev. B **89**, 079904 (2016).

[23] I. S. Burmistrov, I. V. Gornyi, V. Yu. Kachorovskii, M. I. Katsnelson, and A. D. Mirlin, Quantum elasticity of graphene: Thermal expansion coefficient and specific heat, Phys. Rev. B **94**, 195430 (2016).

[24] A. Košmrlj and D. R. Nelson, Statistical Mechanics of Thin Spherical Shells, Phys. Rev. X **7**, 011002 (2017).

[25] P. Le Doussal and L. Radzihovsky, Anomalous elasticity, fluctuations and disorder in elastic membranes, Ann. Phys. (N.Y.) **392**, 340 (2018).

[26] I. S. Burmistrov, V. Yu. Kachorovskii, I. V. Gornyi, and A. D. Mirlin, Differential Poisson's ratio of a crystalline two-dimensional membrane, Ann. Phys. (N.Y.) **396**, 119 (2018).

[27] I. S. Burmistrov, I. V. Gornyi, V. Yu. Kachorovskii, M. I. Katsnelson, J. H. Los, and A. D. Mirlin, Stress-controlled Poisson ratio of a crystalline membrane: Application to graphene, Phys. Rev. B **97**, 125402 (2018).

[28] D. R. Saykin, I. V. Gornyi, V. Yu. Kachorovskii, and I. S. Burmistrov, Absolute Poisson's ratio and the bending rigidity exponent of a crystalline two-dimensional membrane, Ann. Phys. (N.Y.) **414**, 168108 (2020).

[29] O. Coquand, D. Mouhanna, and S. Teber, The flat phase of polymerized membranes at two-loop order, Phys. Rev. E **101**, 062104 (2020).
[30] A. Mauri and M. I. Katsnelson, Scaling behavior of crystalline membranes: an ϵ-expansion approach, Nucl. Phys. **B956**, 115040 (2020).
[31] A. Mauri and M. I. Katsnelson, Scale without conformal invariance in membrane theory, Nucl. Phys. **B969**, 115482 (2021).
[32] J. Toner, Elastic Anisotropies and Long-Ranged Interactions in Solid Membranes, Phys. Rev. Lett. **62**, 905 (1989).
[33] *Statistical Mechanics of Membranes and Surfaces*, edited by D. Nelson, T. Piran, and S. Weinberg(World Scientific, Singapore, 1989).
[34] L. Radzihovsky and J. Toner, A New Phase of Tethered Membranes: Tubules, Phys. Rev. Lett. **75**, 4752 (1995).
[35] M. Bowick, M. Falcioni, and G. Thorleifsson, Numerical Observation of a Tubular Phase in Anisotropic Membranes, Phys. Rev. Lett. **79**, 885 (1997).
[36] L. Radzihovsky and J. Toner, Elasticity, shape fluctuations, and phase transitions in the new tubule phase of anisotropic tethered membranes, Phys. Rev. E **57**, 1832 (1998).
[37] K. Essafi, J.-P. Kownacki, and D. Mouhanna, Crumpled-to-Tubule Transition in Anisotropic Polymerized Membranes: Beyond the ϵ Expansion, Phys. Rev. Lett. **106**, 128102 (2011).
[38] Here a "prime" sign in the last integral indicates that the interaction with $q = 0$ is excluded. Also we omit the so-called zero-mode contribution to $\mathcal{F}$.
[39] E. Cadelano, P. L. Palla, S. Giordano, and L. Colombo, Elastic properties of hydrogenated graphene, Phys. Rev. B **82**, 235414 (2010).
[40] Q. Wei and X. Peng, Superior mechanical flexibility of phosphorene and few-layer black phosphorus, Appl. Phys. Lett. **104**, 251915 (2014).
[41] See Supplemental Material at http://link.aps.org/supplemental/10.1103/PhysRevLett.128.096101 for details of derivation of Eq. (4), absence of renormalization of γ, the anomalous Hooke's law, and the flat–to–tubule transition temperature.
[42] I. V. Gornyi, V. Yu. Kachorovskii, and A. D. Mirlin, Rippling and crumpling in disordered free-standing graphene, Phys. Rev. B **92**, 155428 (2015).
[43] A. Tröster, Fourier Monte Carlo simulation of crystalline membranes in the flat phase, J. Phys. **454**, 012032 (2013).
[44] L. Wang, A. Kutana, X. Zou, and B. I. Yakobson, Electro-mechanical anisotropy of phosphorene, Nanoscale **7**, 9746 (2015).
[45] H.-Y. Zhang and J.-W. Jiang, Elastic bending modulus for single-layer black phosphorus, J. Phys. D **48**, 455305 (2015).
[46] R. J. T. Nicholl, H. J. Conley, N. V. Lavrik, I. Vlassiouk, Y. S. Puzyrev, V. P. Sreenivas, S. T. Pantelides, and K. I. Bolotin, The effect of intrinsic crumpling on the mechanics of free-standing graphene, Nat. Commun. **6**, 8789 (2015).
[47] J.-W. Jiang and H. S. Park, Negative poisson's ratio in single-layer black phosphorus, Nat. Commun. **5**, 4727 (2014).
[48] Y. Du, J. Maassen, W. Wu, Z.Luo, X. Xu, and P. D. Ye, Auxetic black phosphorus: A 2D material with negative Poisson's ratio, Nano Lett. **16**, 6701 (2016).
[49] A. N. Rudenko, S. Brener, and M. I. Katsnelson, Intrinsic Charge Carrier Mobility in Single-Layer Black Phosphorus, Phys. Rev. Lett. **116**, 246401 (2016).
[50] S. Brener, A. N. Rudenko, and M. I. Katsnelson, Effect of flexural phonons on the hole states in single-layer black phosphorus, Phys. Rev. B **95**, 041406(R) (2017).
[51] P. Le Doussal and L. Radzihovsky, Thermal Buckling Transition of Crystalline Membranes in a Field, Phys. Rev. Lett. **127**, 015702 (2021).
[52] D. R. Nelson and L. Radzihovsky, Polymerized membranes with quenched random internal disorder, Europhys. Lett. **16**, 79 (1991).
[53] L. Radzihovsky and D. R. Nelson, Statistical mechanics of randomly polymerized membranes, Phys. Rev. A **44**, 3525 (1991).
[54] D. C. Morse, T. C. Lubensky, and G. S. Grest, Quenched disorder in tethered membranes, Phys. Rev. A **45**, R2151(R) (1992).
[55] D. C. Morse and T. C. Lubensky, Curvature disorder in tethered membranes: A new flat phase at $t = 0$, Phys. Rev. A **46**, 1751 (1992).
[56] D. Bensimon, D. Mukamel, and L. Peliti, Quenched curvature disorder in polymerized membranes, Europhys. Lett. **18**, 269 (1992).
[57] A. Košmrlj and D. R. Nelson, Mechanical properties of warped membranes, Phys. Rev. E **88**, 012136 (2013).
[58] A. Košmrlj and D. R. Nelson, Thermal excitations of warped membranes, Phys. Rev. E **89**, 022126 (2014).
[59] I. V. Gornyi, V. Yu. Kachorovskii, and A. D. Mirlin, Anomalous Hooke's law in disordered graphene, 2D Mater. **4**, 011003 (2016).
[60] O. Coquand, K. Essafi, J.-P. Kownacki, and D. Mouhanna, Glassy phase in quenched disordered crystalline membranes, Phys. Rev. E **97**, 030102(R) (2018).
[61] D. R. Saykin, V. Yu. Kachorovskii, and I. S. Burmistrov, Phase diagram of a flexible two-dimensional material, Phys. Rev. Research **2**, 043099 (2020).